Adsorption (2019) 25:1057–1066
https://doi.org/10.1007/s10450-019-00061-1

The first evaluation of the dynamic hydration number of hydrated ions confined in mesoporous silica MCM-41

Ryota Ogura[1] · **Takahiro Ueda**[1,2]

Received: 1 December 2018 / Revised: 15 February 2019 / Accepted: 13 March 2019 / Published online: 21 March 2019

Abstract
Ion hydration in narrow pores is important in engineering, biology, and chemistry. The structures of hydrated ions confined in nanospaces have been studied by X-ray diffraction and X-ray absorption spectroscopy, and these confined hydrated ions have been found to have anomalous structures. On the other hand, the dynamic behavior has been studied only by molecular dynamics (MD) simulations, which have revealed the unique dynamics of hydration in nanospaces. However, no experimental studies of the dynamics of confined hydrated ions have been carried out. Here, we focus on the dynamic hydration number (n_{DHN}) used in bulk solutions to evaluate the dynamic behavior of electrolyte solutions confined in nanospaces. To evaluate n_{DHN} in nanospaces, we derived the molality dependence of the ^{2}H spin–lattice relaxation time of D_2O confined in nanospaces by considering the contribution of water bound to the pore surface. Next, we applied this to electrolyte solutions confined in mesoporous silica MCM-41 and evaluated n_{DHN}. The absolute value of the dynamic hydration number in mesopores is significantly larger than that in the bulk solution; thus, the confinement effect drastically enhances the dynamic hydration properties (positive and negative hydration). This result supports the compressed hydration structure of ions with positive hydration character reported by previous structural and simulation studies. Our new approach for the evaluation of n_{DHN} in nanospaces can be expected to give new insights in the investigation of electrolyte solutions confined in nanospaces from the viewpoint of the experimental verification of dynamic features of the hydration structure.

Keywords Dynamic hydration number · Hydration · ^{2}H-NMR · Confinement · Electrolyte solution

1 Introduction

There is growing interest in the structure and physical properties of hydrated ions confined in nanospaces because their hydration structure and properties are different to those in bulk solution. The unique structure and properties of ions play an important role in the fundamental processes in electrolyte solutions such as ion transport, the formation of the electric bilayer, and charge/energy storage. In addition, the hydration structure in the nanospace has attracted much attention from an engineering viewpoint because it is related to the capacitance of electric double layer capacitors (EDLC) (Chmiola et al. 2006, 2008; Kalluri et al. 2013; Icaza and Guduru 2016), as well as ion transport through ion channels in biological membranes (Pfeifer et al. 2006; Zhou et al. 2001; Yu et al. 2009; Richards et al. 2012; Hinkle et al. 2016).

From the microscopic viewpoint, the electrochemical properties and the ion transport behavior are closely related to the specific and unique structure and properties of the hydrated ions confined in the nanospace. For example, Kalluri et al. (2013) underlined the importance of the size of electrolyte ions with respect to the pore size of the electrodes for increasing the capacitance of EDLCs (Icaza and Guduru 2016). Chmiola et al. (2006, 2008) also reported a mechanism in which the removal of the solvent shell leads to some form of charge/energy storage. Furthermore, in biological systems, the topological control hypothesis presented by Bostick and Brooks (2007) has attempted to explain the binding selectivity in potassium channels based on the premise that a universal measure of ion solvation in different environments is provided by the average coordination structure in bulk water. In this context, Yu et al. (2009) reported that

✉ Takahiro Ueda
ueda@museum.osaka-u.ac.jp

[1] Department of Chemistry, Graduate School of Science, Osaka University, Toyonaka, Osaka 560-0043, Japan

[2] The Museum of Osaka University, Osaka University, Toyonaka, Osaka 560-0043, Japan

ion selectivity is predominantly controlled by the number of ligands coordinating the ion. In addition, in the so-called "nanosolution" confined in the nanospace, the viscosity of the hydration water confined in a thickness of 0.7–1.35 nm is about 5–16 times larger than the bulk value (that is, the ordered structuring of water is increased) (Leng 2008). Furthermore, Malan et al. (2006) reported that the solubility of NaCl in water is reduced by a factor of two within 0.8 nm slits. Thus, the hydration structure of ions, including the dehydration and the variation of the hydration number, is one of the most basic and significant factors affecting the physicochemical properties of confined electrolyte solutions.

The hydration structure has been studied experimentally using X-ray absorption techniques such as X-ray absorption fine structure (XAFS) and extended X-ray absorption fine structure (EXAFS) spectroscopy. Ohkubo et al. (2002) reported the structure of the hydrated ions of Rb^+, Ca^{2+}, Cu^{2+}, Co^{2+}, and Zn^{2+} confined in carbon nanotubes (CNT) and activated carbon (AC) (Ohkubo et al. 2002, 2003, 2012, 2011; Ahmmad et al. 2013; Nishi et al. 2013). They found that dehydration (decrease in the hydration number) occurred and a compact hydrated structure formed for Co^{2+} and Zn^{2+} in CNTs and Rb^+ and Zn^{2+} in AC with a slit-width less than the total diameter of the symmetrically hydrated ion. In addition, they found that Ca^{2+} ions formed a distorted non-spherically-symmetric hydration shell in carbon micropores with a size of 1 nm (Ohkubo et al. 2016). Furthermore, Ohba et al. (2012), Ohba (2014) also studied the structure of hydrated Na^+ ions confined in CNTs by a combination of X-ray diffraction (XRD) and computational methods such as molecular dynamics (MD) and Monte Carlo simulations (Oya et al. 2017). They found that an anomalously strong hydration shell formed, decreasing the intermolecular separation between the water molecules in the electrolyte solution and weakening the water correlation at second-neighbor or longer distances (Ohba et al. 2012; Ohba 2014). In addition, the hydration structure of the ions in the CNTs depends on the diameter of the nanotubes. For the nearest-neighbor distance between ions and water molecules, anomalously longer distances were observed in electrolytes in 1 nm diameter CNT; in contrast, in 2 and 3 nm CNT, shorter nearest-neighbor distances were observed than those in the bulk electrolyte (Oya et al. 2017). Urita et al. (2014) also studied the solvated states of Li^+ ions in confined carbon micropores using Raman spectroscopy and ^7Li NMR, finding a decrease in the solvation number and an increase in the specific capacitance in these confined solutions. These specific and unique structures of the hydrated ions have also been studied extensively by MD and Monte Carlo simulations. MD simulations reveal the enhancement in the interaction between cations (Na^+ and K^+) and the water molecules in CNT(8,8) at 300 K, whereas the interactions are similar or weaker than that in the bulk in CNT(n,n) (n = 6, 7, 9 and 10) (Zhu et al. 2010; He et al. 2013). Under an external electric field (E) of 0–0.1 V/nm, the coordination number in the first hydration shell of Na^+ ions inside CNTs increases with increasing E (Wu et al. 2013). Canonical Monte Carlo simulations found a pentagonal hydration structure of Ca^{2+} ions in 0.6 nm pores. In the pores, the Ca^{2+} ions are surrounded by a more tightly hydrogen-bonded shell of water molecules than those in bulk solution, whereas the Cl^- ions have a more diffuse hydration shell than those in the bulk solution (Ohba et al. 2009).

In contrast, the physicochemical properties of electrolyte solutions confined in nanospaces are closely related to the dynamic structures and properties of the hydrated ions such as accumulation, penetration, diffusivity, and transportation of ions in nanopores. To date, the dynamic behaviors of hydrated ions in confined conditions have been studied only by MD simulations (Malan et al. 2006; Leng 2008; Richards et al. 2012; Kalluri et al. 2013; Ohba 2015, 2017; Hou and Li 2018). In particular, Hou and Li (2018) studied a NaCl solution confined in the 5.6 nm slit-shaped nanopores in calcium silicate hydrate gel and found a 50% reduction in the diffusion coefficient of the Na^+ ion and a 40% increase in the hydration time of the Na^+ ions. The penetration of ions in the slit-shaped carbon pores (Kalluri et al. 2013) and dynamic squeeze-out process from the interstices between two mica surfaces (Leng et al. 2008) have also been investigated using MD simulations. Richards et al. (2012) examined the ion transport of anionic drinking water contaminants (fluoride, chloride, nitrate, and nitrite) in pores ranging in effective radius from 0.28 to 0.65 nm using MD to elucidate the role of hydration in excluding these species during nanofiltration. It was found that the partial dehydration of the transported ions is the main contribution to the energy barrier based on analysis of the free-energy profile of the ion transport path, demonstrating the importance of ion dehydration in transport through narrow pores. Ohba (2015, 2017) investigated the ion transport between partially charged conical carbon electrodes and that between charged graphene layers. They found that fast ion transport is accompanied by an increasing hydration number, suggesting the rapid rearrangement of water molecules in the hydration shell. Furthermore, they also suggested that the breaking and reconstruction of the hydrogen bonds of water molecules around the ions are closely related to the fast ion transfer during the charge and discharge cycles.

Thus, the study of the structure of the hydrated ions in the nanopores has been mainly carried out based on the average structure, and the dynamic properties have been investigated only using computer simulation techniques. In particular, the dynamic properties of the hydrated ions are important to understand the dynamic properties of electrolyte solutions, such as the viscosity, conductivity and diffusivity. However, experimental studies of the dynamic hydration structure of

ions confined in a nanospace remain under investigated. Experimental information about the structure and the physical properties of the hydrated ions in nanospaces is expected to bring new insights to science and technology involving nanosolutions. Therefore, our immediate aim is the experimental study of the dynamic hydration structure of ions in confined systems. In general, the mobility of hydrated ions can be evaluated based on the rotational correlation time (τ_c) of hydration water. This is the average time required for molecules to obtain a certain orientation in the rotational motion of the water molecules. In other words, the discussion of the dynamic properties of hydrated ions requires a means to measure τ_c experimentally. However, in the electrolyte solution, water molecules inside and outside the hydration shells exchange rapidly and dynamically, and it is quite difficult to measure τ_c directly. Thus, we focus on the dynamic hydration number n_{DHN} ($=n_{Hyd}[\tau_c^{\pm}/\tau_c^{B}-1]$) introduced by Uedaira et al. (1989), where n_{Hyd} is the average hydration number of ions and $\tau_c^{\pm}$ and τ_c^{B} are the rotational correlation times of hydration and bulk water, respectively. The use of n_{DHN} makes it possible to discuss $\tau_c^{\pm}$, which is challenging to measure directly. Although n_{DHN} can be determined from the concentration dependence of the spin–lattice relaxation time (T_1) from ^{2}H-NMR and ^{17}O-NMR measurements (Uedaira and Uedaira 1986; Uedaira et al. 1989; Shimizu and Taniguchi 1990), it has not yet been measured in nanosolutions confined in nanospaces. To evaluate n_{DHN} in the nanospace, it is necessary to extend the concentration dependence of T_1 in the bulk solution to a formula suitable for the nanospace, thus taking account of the contribution of water molecules bound to the pore walls. In this study, we will derive the formula of the concentration dependence of ^{2}H T_1, thus allowing the analysis of electrolyte solutions confined in nanospaces. By applying the extended formula to the confined solutions in the mesopores of MCM-41, we aim to determine n_{DHN} in confined solutions.

2 Model

The dynamic aspects of the hydration structure of ions are generally discussed based on the concept of positive and negative hydration, as first proposed by Samoilov (1957). This concept represents the relative mobility of hydration water molecules with respect to the motion of bulk water molecules. If the motion becomes slower than that in the bulk, the hydration is denoted "positive hydration", whereas if the motion becomes faster than that in bulk, the hydration is denoted "negative hydration". Focusing on the rotational motion of water molecules, it is possible to discuss positive hydration ($\tau_c^{\pm}/\tau_c^{B}>1$) and negative hydration ($\tau_c^{\pm}/\tau_c^{B}<1$) based on the ratio of the correlation time of bulk and hydration water. The rotational correlation time of water molecule can be examined using the ^{2}H spin–lattice relaxation time (^{2}H T_1). In the extremely narrowing region ($\omega_0\tau_c<<1$: ω_0 is Larmor frequency of ^{2}H nuclei in rad s^{-1} unit), the spin–lattice relaxation rate ($1/T_1$) of ^{2}H nuclei can be related to the rotational correlation time (τ_c) using the Bloembergen–Purcell–Pound (BPP) formula (Abragam 1961):

$$R_1 = 1/T_1 = \frac{3}{8}\left(2\pi\chi_Q\right)^2\left(1+\eta_Q^2/3\right)\tau_c, \tag{1}$$

where χ_Q is the nuclear quadrupole coupling constant (equal to e^2Qq/h), and η_Q is the asymmetry parameter of the electric field gradient (EFG) tensor. In general, the thermal motion of water in both the bulk and in the hydration shell is sufficiently fast to satisfy this condition. In this case, it is convenient to use the dynamic hydration number defined by Uedaira and Uedaira (1986), Uedaira et al. (1989) for a discussion of the dynamic structure of hydration water. Thus, the dynamic hydration number was used as an index of the mobility of the hydration water, as shown in Eq. (2a), where $\nu_{\pm}$ is the charge of ions, $n_{\pm}$ is the hydration number of the ions, $B^{\pm}$ is a constant dependent on each ion, and $\tau_c^{\pm}/\tau_c^{B}$ is the ratio of rotational correlation time of water molecule between hydrated and bulk water. The $B^{\pm}$ values were evaluated from the molality dependence of T_{1B}/T_1, where T_{1B} is the spin–lattice relaxation time of water in the bulk and m is the molality of the solution.

$$n_{DHN}^{\pm} = \nu_{\pm}n_{\pm}\left(\frac{\tau_c^{\pm}}{\tau_c^{B}}-1\right) = 55.5B^{\pm} \tag{2a}$$

$$\frac{T_{1B}}{T_1} = 1+\left(B^{+}+B^{-}\right)m \tag{2b}$$

In the mesopores, the confined D_2O molecules are distributed between surface bound molecules and those in the free space in the pores. Therefore, the observable spin–lattice relaxation rate ($1/T_1^{0}$) is given by the average of the spin–lattice relaxation rates of D_2O occupying two regions (two-region model) (Hwang et al. 2001): the bulk-like region ($1/T'_{1B}$) and surface-bound region ($1/T_{1S}$), and is represented by:

$$\frac{1}{T_1^0} = (1-x_S)\frac{1}{T'_{1B}} + x_S\frac{1}{T_{1S}}, \tag{3}$$

where x_S is the molar fraction of D_2O occupying the surface-bound region. Here, we denote the spin–lattice relaxation rate of D_2O in the bulk-like region as $1/T'_{1B}$ to distinguish it from that of pure bulk D_2O.

For electrolyte solutions confined in the mesopores, the contribution of the relaxation rates ($1/T_{1+}$, $1/T_{1-}$) stemming from the hydrated water of each of cation and anion will be added to the above two contributions. For a dilute solution,

we assume that the D_2O molecules occupying the specific regions (hydrated water and surface-bound water) undergo chemical exchange only with D_2O in the bulk-like region. In this case, the observable spin–lattice relaxation rate ($1/T_1$) for the electrolyte solution confined in the mesopores can be represented by the average of these four terms (four-region model).

$$\frac{1}{T_1} = (1 - x_+ - x_- - x_S)\frac{1}{T'_{1B}} + x_+\frac{1}{T_{1+}} + x_-\frac{1}{T_{1-}} + x_S\frac{1}{T_{1S}} \tag{4}$$

Here, $1/T_{1+}$ and $1/T_{1-}$ are the spin–lattice relaxation rate of D_2O hydrating the cation and the anion, respectively, and x_+ and x_- are the molar fractions of D_2O molecules hydrating cations and anions, respectively. Using Eqs. (3) and (4), we can derive the spin–lattice relaxation rate normalized by that in the bulk-like region:

$$\frac{T'_{1B}}{T_1} = \frac{T'_{1B}}{T_1^0} + x_+\left(\frac{T'_{1B}}{T_{1+}} - 1\right) + x_-\left(\frac{T'_{1B}}{T_{1-}} - 1\right) \tag{5}$$

The molar fraction of D_2O hydrating cations and anions can be given as $n_\pm\nu_\pm m/55.5$, using the hydration number ($n_\pm$) and the valence number ($\nu_\pm$) of each ion and the molality of the solution (m). Furthermore, in extreme narrowing region, the ^2H spin–lattice relaxation rate in D_2O is proportional to the rotational correlation time (τ_c). Thus, Eq. (5) can be rewritten as:

$$\frac{T'_{1B}}{T_1} = \frac{T'_{1B}}{T_1^0} + \left[n_+\nu_+\left(\frac{\tau_c^+}{\tau_c'^B} - 1\right) + n_-\nu_-\left(\frac{\tau_c^-}{\tau_c'^B} - 1\right)\right]\frac{m}{55.5} = \frac{T'_{1B}}{T_1^0} + Bm. \tag{6}$$

As described above, $n_{\mathrm{DHN}}{}^\pm = n_\pm\nu_\pm(\tau_c{}^\pm/\tau_c{}'^B - 1)$. For the analysis of the molality dependence of $1/T_1$, we consider the quadratic term as a higher order term, $T'_{1B}/T_1 = T'_{1B}/T_1{}^0 + Bm + Cm^2$. This term stems from the contribution of the spin–lattice relaxation arising from the translational diffusion in the restricted space (Endom et al. 1967). This term may also arise from the direct exchange of the water molecules between the cationic and the anionic hydration shells and between the hydrated and surface-bound waters. In the bulk solution, the intercept of the molality dependence in the normalized spin–lattice relaxation rate should be 1. On the other hand, in the confined solution, the difference in the spin–lattice relaxation rate between the confined solution and the confined water depends on the molality, and the intercept of the corresponding plot is null. In this study, we apply this approach to NaCl, KCl, and $CaCl_2$ aqueous solutions confined in MCM-41 mesopores to determine the dynamic hydration number (n_{DHN}) of the ions and discuss dynamic structure of hydration water in the mesopores.

3 Experimental

Mesoporous silica MCM-41 and anhydrous $CaCl_2$ were purchased from Sigma-Aldrich Co., LLC. A fresh MCM-41 sample used immediately after purchase is denoted as "MCM-41", and a MCM-41 sample aged for 6 months after purchase is denoted as "the 6-month-aged MCM-41". MCM-41 specimen modified by trimethylsilyl-group is also used for estimation of $1/T'_{1B}$. Trimethylsilylation was conducted according to the literature (Beck et al. 1992), and MCM-41 after trimethylsilylation is denoted by MCM-41-TMS (substitution ratio is 78% of the ideal maximum substitution). Nitrogen adsorption isotherm was used to characterize the porosity of porous materials. The N_2 adsorption isotherms are presented in Fig. 1, from which the pore volume was found to be 0.64 cm^3g^{-1} for MCM-41 and 0.47 cm^3g^{-1} for MCM-41-TMS. The Brunauer–Emmett–Teller (BET) plot indicates that the specific surface area was 840 m^2g^{-1} for MCM-41 and 764 m^2g^{-1} for MCM-41-TMS. The Barrett–Joyner–Halenda (BJH) analysis led to an average pore diameter of 2.67 nm for MCM-41 and 2.38 nm for MCM-41-TMS. KCl and NaCl were purchased from FUJIFILM Wako Pure Chemical Corporation. Deuterium oxide was supplied from Tokyo Chemical Industry Co., Ltd. (99.8 atm%) and Cambridge Isotope Laboratories, Inc. (99.96 atm%). MCM-41 samples adsorbing KCl, NaCl, and $CaCl_2$ heavy water solutions were prepared according

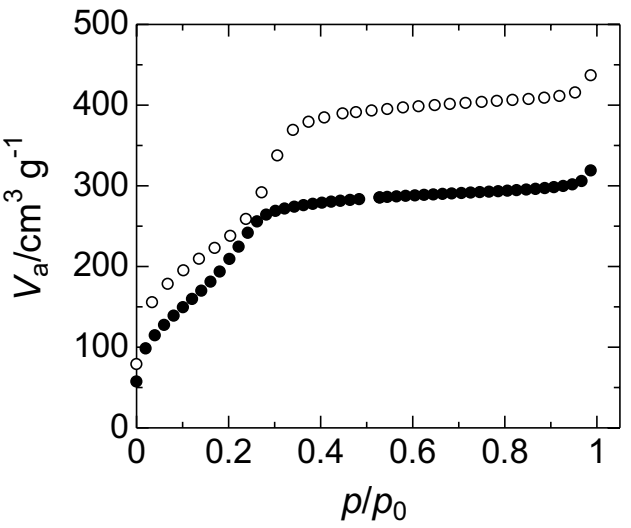

Fig. 1 N_2 adsorption isotherm for MCM-41 (circle) and MCM-41-TMS (filled circle). The both results show the typical type-IV adsorption isotherm based on the IUPAC classification, indicating the presence of mesopores

to the following procedure: First, the MCM-41 specimen was pretreated by evacuation under reduced pressure (10^{-2} Torr) for 6 h at 473 K. Then, the heavy water solution with an appropriate molality corresponding to the pore volume was added to the pretreated MCM-41 specimen and sealed into a glass ampoule (5 mmφ × 25 mm lengths) after deoxygenation. The sealed ampoules were agitated using a vortex mixer (1000 rpm) for 16 h. The bulk KCl, NaCl, and $CaCl_2$ solutions were also prepared in the same procedure but without MCM-41. Thermogravimetric (TG)–differential thermal analysis (DTA) measurements were carried out for the MCM-41 samples saturated with pure H_2O and KCl solutions ($m = 1$ mol kg^{-1}). Below 100 °C, the TG diagram showed the weight loss of the samples corresponding to H_2O in the mesopores. The amount of desorption was less than the loaded amount, suggesting that some of the water molecules were bound to the pore surface. The ratios of desorbed water were 0.80 and 0.83 for pure H_2O and the KCl solution, respectively, implying that the water molecules represent about 20% of the loaded content of H_2O (or solution) adsorbed on the surface of the pore wall in MCM-41.

^{2}H-NMR experiments were conducted using a Chemagnetics CMX Infinity 300 solid-state NMR spectrometer (^{2}H resonance frequency; 46.127 MHz, $B_0 = 7.06$ T). The ^{2}H spin–lattice relaxation rate ($1/T_1$) was measured at room temperature (298 K) using an inversion–recovery pulse sequence [180° − τ − 90° − acqu.] with a 90° pulse of 3 μs. The repetition time was 5 s and the free induction decay (FID) signals with 2018 sampling points (40 μs of dwell time and 81.92 ms of acquisition time) were accumulated over 16 scans. The ^{2}H magnetization was recovered exponentially, providing a unique spin–lattice relaxation time for each specimen. Examples of the ^{2}H magnetization recovery curves are shown in Fig. 2.

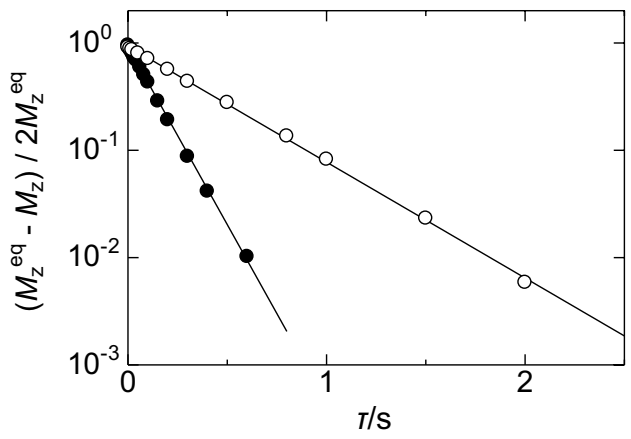

Fig. 2 The typical recovery curves of the ^{2}H magnetization for D_2O: bulk (circle) and D_2O confined in MCM-41(filled circle)

4 Results and discussion

The ^{2}H spin–lattice relaxation rates ($1/T_1$) for bulk D_2O, the bulk solution, and the confined solution are summarized in Table 1. For bulk D_2O, the $1/T_1$ value directly provides the rotational correlation time (τ_c) of the D_2O molecules via Eq. (1). Assuming that the nuclear quadrupole coupling constant and the EFG asymmetry parameter of ^{2}H nuclei in D_2O are 256 kHz and 0.164 (Eggenberger et al. 1992), the $1/T_1$ values of 2.38 and 2.16 s^{-1} give rotational correlation times (τ_c) of 2.43 and 2.21 ps, respectively. These experimental values are coincident with those reported in the literature (2.38 ps at 25 °C) (Shimizu and Taniguchi 1990) within errors of 2% and 7%, respectively, suggesting that the measurements of $1/T_1$ are valid.

In the bulk solution, the observed $1/T_1$ value in the KCl solution decreases, whereas the observed $1/T_1$ values in NaCl and $CaCl_2$ solutions increase with increasing molality. This result suggests that the mobility of the D_2O molecules is higher in the KCl solution and lower in both the

Table 1 ^{2}H spin–lattice relaxation rates in bulk D_2O and confined solutions

Specimen	m/mol kg^{-1}	T_1^{-1}/s^{-1}	
		Bulk	Confined
D_2O[a]	–	2.38	7.89
D_2O[b]	–	2.16	4.67
D_2O[c]	–	2.16	5.26
KCl sol.[a]	0.1	2.37	7.84
	0.5	2.33	–
	1	2.29	6.80
	1.5	2.22	5.95
	2	2.19	5.05
NaCl sol.[a]	0.1	2.38	7.95
	0.5	2.42	8.19
	1	2.46	8.27
	1.5	2.49	–
	2	2.54	8.49
$CaCl_2$ sol.[b]	0.1	2.26	5.03
	0.5	2.42	5.97
	1	2.60	6.69
	1.5	2.81	–
	2	3.11	7.25

[a]Experiment was conducted using D_2O supplied from Tokyo Chemical Industry Co., Ltd. (99.8 atm%) and a fresh MCM-41 sample used immediately after purchase

[b]Experiment was conducted using D_2O supplied from Cambridge Isotope Laboratories, Inc. (99.96 atm%) and an MCM-41 sample aged for 6 months after purchase

[c]Experiment was conducted using D_2O supplied from Cambridge Isotope Laboratories, Inc. (99.96 atm%) and an MCM-41-TMS sample

NaCl and $CaCl_2$ solutions than that in pure bulk D_2O. This result is consistent with the negative hydration ($\tau_c^+/\tau_c^B < 1$) of the K^+ ion and the positive hydration ($\tau_c^+/\tau_c^B > 1$) of the Na^+ and Ca^{2+} ions. Using Eq. (2b), we can evaluate the dynamic hydration number of each ion. Figure 3 shows a plot of T_{1B}/T_1 against the molality of each solution. The B values were determined by optimization of Eq. (2b), thus yielding the dynamic hydration numbers (n_{DHN}) of each ion. The resultant parameters obtained from the optimization, as well as the resultant n_{DHN} values, are listed in Table 2. Because the dynamic properties of K^+ and Cl^-, such as equivalent conductivity, are almost equal, to date, it has been assumed that these ions have same dynamic hydration number (Endom et al. 1967). In this study, our analysis also followed the previous procedure. The obtained n_{DHN} values for all ions are somewhat smaller than those reported in the literature (Uedaira and Uedaira 1986; Endom et al. 1967), but the trend in the magnitude is consistent with that previously reported.

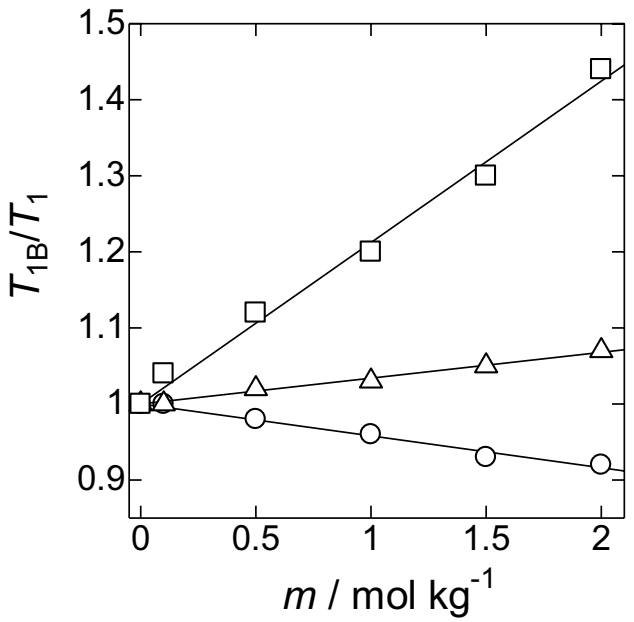

Fig. 3 The molality dependence of the ratio of the ^2H spin–lattice relaxation time in bulk pure D_2O to that in the bulk solutions (T_{1B}/T_1) for KCl (circle),NaCl (triangle), and $CaCl_2$ (square). The solid lines represent the result of optimization using Eq. (2b)

Pure D_2O confined in MCM-41 gave a larger value in $1/T_1^0$ than that in the bulk ($1/T_{1B}$), suggesting a contribution of the surface-bound D_2O molecules as well as confinement effect. Other electrolyte solutions also showed the increase in $1/T_1$ on confinement. Furthermore, significant line broadening in the ^2H-NMR spectrum was observed, as shown in Fig. 4. Although some of the line broadening may be caused by the inhomogeneity of the volume susceptibility of the powdered MCM-41 sample, the broadening mainly arises because of the slowdown of the motion of the confined water molecules. In particular, in the $CaCl_2$ solution, the effect of the line broadening seems to be remarkable, indicating the effective hydration of the Ca^{2+} ion in both bulk and the confined system. According to Eq. (3), the observed $1/T_1^0$ is a result of the averaging of $1/T'_{1B}$ and $1/T_{1S}$. If the $1/T'_{1B}$ value is approximately equal to that in bulk water ($1/T_{1B}$) and the $1/T_{1S}$ value is known, Eq. (3) can be used to find the region of surface bound water (x_S). The rotational correlation time (τ_c^S) of surface bound water in MCM-41, which depends on the water content, has been reported to be 20–60 ps by Hwang et al. (2001) using ^2H double-quantum-filtered NMR measurements. Furthermore, the $1/T'_{1B}$ value is expected to be commonly larger than that of bulk water ($1/T_{1B}$), because confinement effect brings about the slowdown of the motion of the water molecules in the mesopores (Takahara et al. 1999). Thus, in this work, we evaluated the $1/T'_{1B}$ value experimentally to be 5.26 s^{-1} as the $1/T_1^0$ value of D_2O confined in the MCM-41-TMS hydrophobic mesopores, in which a contribution of the surface-bound D_2O molecules is negligible. Based on this $1/T'_{1B}$ value and the fraction of the surface bound water evaluated from TG-DTA measurements ($x_S = 0.2$), we can estimate $1/T_{1S}$ to be 18.4 s^{-1} and 2.31 s^{-1},

Table 2 The dynamic hydration number (n_{DHN}) determined from the T_{1B}/T_1 and $T'_{1B}/T_1 - T'_{1B}/T_1^0$ plots against the molality of the solution

System	Ion	B/mol^{-1} kg	C/mol^{-2} kg^2	n_{DHN} (exp.)	n_{DHN} (references)	$\tau_c^{\pm}$/ps
Bulk	K^+	−0.04194[a]	–	−1.2	−1.21[b]	1.9
	Cl^-	−0.04194[a]	–	−1.2	−1.21[b]	1.9
	Na^+	0.03396	–	3.1	4.1[b]	3.6
	Ca^{2+}	0.2123	–	13	15.0[c]	5.0
Confined	K^+	−0.1509[a]	-6.026×10^{-2}	−4.2	–	1.6
	Cl^-	−0.1509[a]	-6.026×10^{-2}	−4.2	–	1.6
	Na^+	0.1043	-2.399×10^{-2}	10	–	14
	Ca^{2+}	0.5473	-1.516×10^{-1}	35	–	21

[a]It is assumed that B^+ and B^- for KCl in the confined system and that in the bulk solution are equal

[b]Uedaira and Uedaira (1986)

[c]Endom et al. (1967)

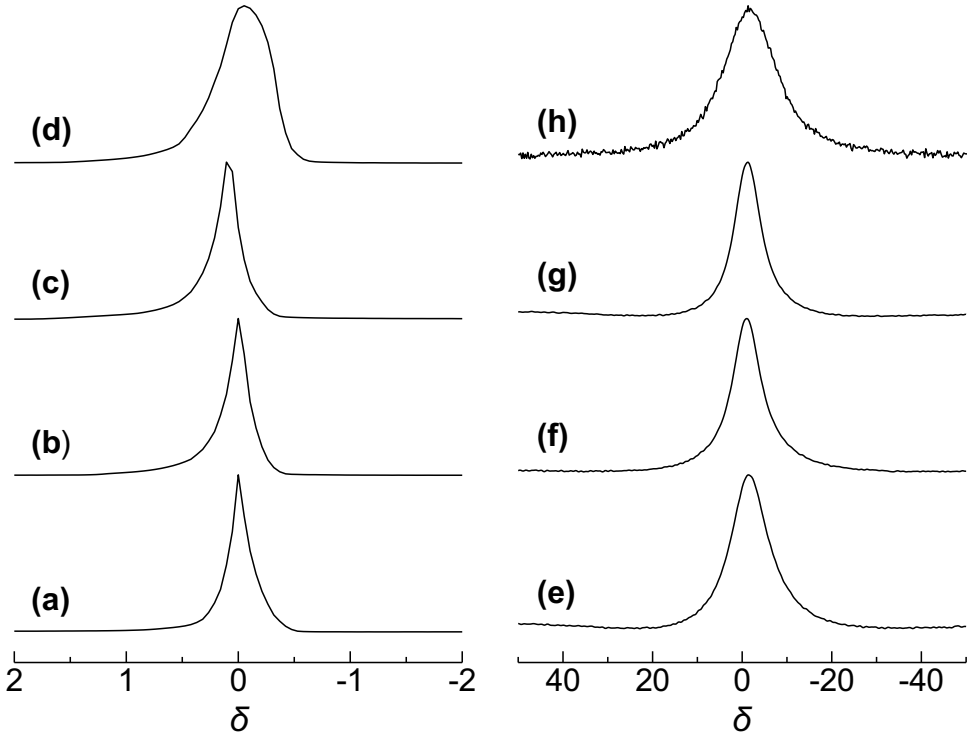

Fig. 4 ^{2}H-NMR spectra of D_2O in the bulk (**a**–**d**) and confined solution (**e**–**h**): bulk D_2O (**a**), bulk KCl solution (**b**), bulk NaCl solution (**c**), bulk $CaCl_2$ solution (**d**), confined D_2O (**e**), confined KCl solution (**f**), confined NaCl solution (**g**), and confined $CaCl_2$ solution (**h**). The concentrations of all solutions were 1 mol kg^{-1}

which corresponds to τ_c^S of 19 ps and 2.4 ps, for the fresh and the 6-months-aged MCM-41 samples, respectively. In the fresh MCM-41 specimen, the estimated τ_c^S of 19 ps is well agreement with 20 ps reported by Hwang et al. (2001), whereas in the 6-months-aged MCM-41 specimen τ_c^S of 2.4 ps is similar to that of bulk water. Unfortunately, the origin of the increase in the mobility of the surface-bound D_2O molecule has not yet been clarified. However, the long-term exposure of MCM-41 sample to humid air will destroy a part of the surface, resulting in the increase in surface roughness. One of the possibilities is that the increase in surface roughness of the pore wall obstructs the formation of hydrogen bonding network between the surface-bound D_2O molecules, facilitating the molecular rotation.

Figure 5 shows the molality dependence of $T'_{1B}(1/T_1 - 1/T_1^0)$ for KCl, NaCl, and $CaCl_2$ solutions confined in MCM-41. In the mesopores of MCM-41, the T'_{1B}/T_1 values of each solution depends on the molality, which is higher than that in the bulk solution, but the trend was more pronounced with KCl. In this case, the plot of $T'_{1B}(1/T_1 - 1/T_1^0)$ against the molality seems to deviate from a linear relationship. Therefore, we considered an additional term of the second order of the molality for the analysis. This contribution may stem from the translational motion of D_2O, which shows little contribution to T_1 in the bulk. On the surface of the pore walls of MCM-41, the anisotropic environment of the D_2O molecule will result in an effective and finite EFG, of which the principal axis value depends on the position of D_2O molecules from the pore

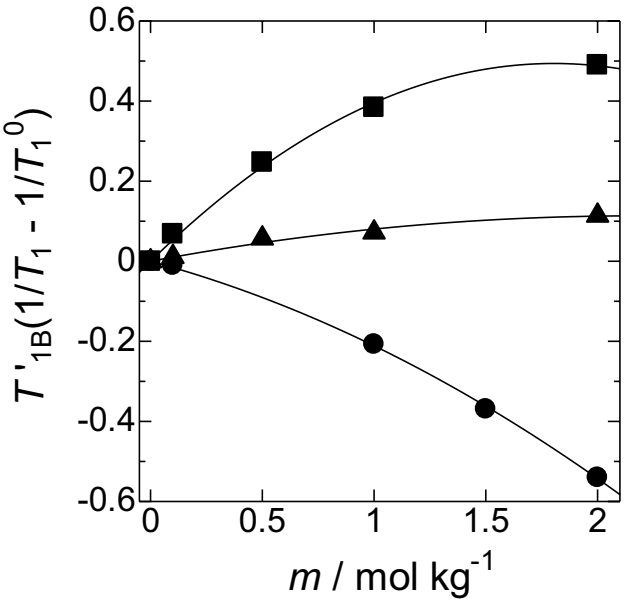

Fig. 5 The molality dependence of the difference between the ratio of the ^{2}H spin–lattice relaxation time (T'_{1B}) of bulk-like D_2O in MCM-41-TMS to that (T_1) in the confined solution and the ratio to that (T_1^0) in confined pure D_2O, $T'_{1B}/T_1 - T'_{1B}/T_1^0$, for KCl (filled circle), NaCl (filled triangle), and $CaCl_2$ (filled square). The solid lines represent the result of optimization using Eq. (6) including the quadratic term (Cm^2)

wall (Ueda et al. 2010). Thus, a D_2O molecule will "feel" a different EFG each time on migration, and the fluctuation of the EFG tensor will contribute to the finite ^2H T_1 in D_2O. Furthermore, the direct exchange between the hydrated water molecules and the hydrated and surface-bound water molecules may also contribute quadratically to the molality dependence of T'_{1B}/T_1. Using Eq. (6), which contains a quadratic term, we optimized the data for each electrolyte. The resultant parameters for data optimization are summarized in Table 2. From the B value, we successfully evaluated the dynamic hydration numbers of the confined ions in MCM-41. The obtained values are also listed in Table 2. At this time, we make an assumption that the n_{DHN} values of K^+ and Cl^- are equal each other, just as with bulk solution. For each of the dynamic hydration numbers, the absolute value was larger than that of the bulk, suggesting that both positive and negative hydration become stronger in the mesopores of MCM-41. This finding suggests that, for the positively hydrated ions, the interaction between the ions and the water molecules is enhanced to a greater extent than that in the bulk, whereas, for the negatively hydrated ions, the interaction between the ions and the water molecules becomes more fragile than that in bulk. This is consistent with the hydration structure previously reported such as the compact hydrated structure of various ions confined in CNTs and activated carbon filters (ACFs) Co^{2+} and Zn^{2+} in CNT, Rb^+ and Zn^{2+} in AC (Ohkubo et al. 2002, 2003, 2011, 2012; Ahmmad et al. 2013; Nishi et al. 2013) and the anomalously strong hydration shell of Na^+ in CNTs (Ohba et al. 2012), Ohba (2014). The enhancement of the positive and the negative hydration for Ca^{2+} and Cl^- ions also supports the result that a pentagonally hydrated Ca^{2+} ion is surrounded by a more tightly hydrogen-bonded shell of water than that in the bulk solution, whereas Cl^- ions have a more diffuse hydration shell than those in the bulk solution (Ohba et al. 2009), as observed by canonical Monte Carlo simulation. Furthermore, in the dynamic behavior of the hydrated ions, the slowdown of the water molecules hydrating the Na^+ ions is consistent with the fact that the diffusion coefficient of the Na^+ ion decreases and the hydration lifetime increases in NaCl solutions confined in calcium silicate hydrate gel (Hou and Li 2018). Thus, the procedure for determining the n_{DHN} value proposed in this study is valid for mesopores.

Based on the resultant dynamic hydration numbers, we can discuss the dynamic structure of the hydrated ions in both the bulk and the confined solutions. In bulk solution, Na^+ and Ca^{2+} show positive hydration, whereas K^+ and Cl^- show negative hydration. In comparison with bulk water, the water molecules occupying the hydration shell of the Na^+ and Ca^{2+} ions rotate slower and those of the K^+ and Cl^- ions rotate faster. To evaluate the ratio of the rotational correlation time, $\tau_c^{\pm}/\tau_c'^{B}$, it is necessary to find the hydration number of each ion in the mesopores of MCM-41. However, although the hydration number of each ion changes in the narrow pores (Zhu et al. 2010; Wu et al. 2013; Ohba 2015; Qiu et al. 2016), the hydration numbers of each ion have not yet been clarified experimentally in MCM-41. Therefore, to advance our discussion, we assume that the hydration number of each ion in MCM-41 is same as typical hydration number in the bulk ($\eta_{\pm}=6$) (Mähler and Persson 2012). The $\tau_c^{\pm}/\tau_c'^{B}$ value was evaluated to be 2.7, 3.9, 0.3 and 0.3 for Na^+, Ca^{2+}, K^+ and Cl^-, respectively, in MCM-41. Using $\tau_c'^{B}=5.37$ ps, the $\tau_c^{\pm}$ values are evaluated as listed in Table 2. The correlation times become 3.9–4.2 times longer around the positive hydration ions, whereas it is 0.84-times shorter around the negative hydration ions, in comparison with those in bulk solution. That is, the confinement brings about a more constructive hydration of Na^+ and Ca^{2+} and more destructive hydration of K^+ and Cl^- in MCM-41. This trend is consistent with the results of the Monte Carlo simulation of aqueous $CaCl_2$ solutions reported by Ohba et al. (2009). The present report is first experimental report of the enhancement in both positive and negative hydration in confined systems. Finally, we note the fact that the reduction in τ_c for the negative hydration ions is much smaller than increment in τ_c for the positive hydration ions, being possibility inclusion of a large uncertainty in the evaluated τ_c. This may result in the physical requirement that $\tau_c^{\pm}/\tau'^{B}_c>0$. That is, the molality dependence of $1/T_1$ is not sufficiently sensitive to detect the small change in $\tau_c^{\pm}/\tau'^{B}_c$ in the range of $0<\tau_c^{\pm}/\tau'^{B}_c<1$ (negative hydration). Therefore, our approach is considered to be effective for the evaluation of $\tau_c^{\pm}/\tau'^{B}_c>1$ (positive hydration).

5 Conclusion

To allow the study of the dynamic properties of hydrated ions in nanopores, we examined the possibility of using the dynamic hydration number, n_{DHN}. First, we modified the molality dependence of the ^2H spin–lattice relaxation rate for the bulk solution to derive an appropriate formula for the confined solution systems. In particular, we have taken account of the contribution of the surface bound water to the relaxation times.

Next, we applied the derived formula to the molality dependence of the ^2H spin–lattice relaxation times for electrolyte solutions (KCl, NaCl, and $CaCl_2$) confined in the mesopores of MCM-41. By examining the molality dependence of ^2H T_1 carefully for each electrolyte, we can determine the n_{DHN} values for K^+, Na^+, Ca^{2+}, and Cl^- in MCM-41. Furthermore, it was found that the magnitude of the n_{DHN} values (absolute value of n_{DHN}) is effectively increased by confinement. This means that there is an enhancement in the dynamic hydration properties, so-called "positive and negative hydration character," in the mesopores. This result

is consistent with the previous structural studies by XAFS, EXAFS, and XRD. Furthermore, this experimental finding also supports the picture of hydrated ions confined in CNTs and ACFs based on MD and MC simulations.

However, the evaluated n_{DHN} values indicate a small reduction in the τ_c of K^+ and Cl^- ions, which leads a large relative error. Thus, the proposed approach for the determination of n_{DHN} in the confined system seems to be more effective for positively hydrated ions with $\tau_c^{\pm}/\tau'^{B}_c > 1$ than for negatively hydrated ions with $0 < \tau_c^{\pm}/\tau'^{B}_c < 1$.

Furthermore, to discuss $\tau_c^{\pm}/\tau'^{B}_c$ more quantitatively, the average hydration number of ions confined in the nanopores is required, which could be obtained from structural studies such as XAFS, EXAFS, and XRD. The combination of our approach with other structural methods giving the hydration number will allow the study of the dynamic behavior of hydration water in confined solutions.

Acknowledgements The authors thank Dr. Naoya Inazumi and Dr. Yasuto Todokoro of the Analytical Instrument Facility, Graduate School of Science, Osaka University for their helpful and useful advice, guidance, and instructions concerning NMR measurements.

References

Abragam, A.: Principles of nuclear magnetism. Oxford University Press, Oxford (1961)

Ahmmad, B., Nishi, M., Hirose, F., Ohkubo, T., Kuroda, Y.: Structure of hydrated cobalt ions confined in the nanospace of single-walled carbon nanotubes. Phys. Chem. Chem. Phys. **15**, 8264–8270 (2013)

Beck, J.S., Vartuli, J.C., Roth, W.J., Leonowicz, M.E., Kresge, C.T., Schmitt, K.D., Chu, C.T.W., Olson, D.H., Sheppard, E.W., McCullen, S.B., Higgins, J.B., Schlenker, J.L.: A new family of mesoporous molecular sieves prepared with liquid crystal templates. J. Am. Chem. Soc. **114**, 10834–10843 (1992)

Bostick, D.L., Brooks, C.L. III: Selectivity in K^+ channels is due to topological control of the permeant ion's coordinated state. Proc. Natl. Acad. Sci. USA **104**, 9260–9265 (2007)

Chmiola, J., Yushin, G., Gogotsi, Y., Portet, C., Simon, P., Taberna, P.L.: Anomalous increase in carbon capacitance at pore sizes less than 1 nanometer. Science **313**, 1760–1763 (2006)

Chmiola, J., Largeot, C., Taberna, P.L., Simon, P., Gogotsi, Y.: Desolvation of ions in subnanometer pores and its effect on capacitance and double-layer theory. Angew. Chem., Int. Ed. **47**, 3392–3395 (2008)

Eggenberger, R., Gerber, S., Huber, H., Searles, D., Welker, M.: Ab initio calculation of the deuterium quadrupole coupling in liquid water. J. Chem. Phys. **97**, 5898–5904 (1992)

Endom, L., Hertz, H.G., Thül, B., Zeidler, M.D.: A microdynamic model of electrolyte solutions as derived from nuclear magnetic relaxation and self-diffusion data. Ber. Bunsenges. Phys. Chem. **71**, 1008–1031 (1967)

He, Z., Zhou, J., Lu, X., Corry, B.: Ice-like water structure in carbon nanotube (8,8) induces cationic hydration enhancement. J. Phys. Chem. C **117**, 11412–11420 (2013)

Hinkle, K.R., Jameson, C.J., Murad, S.: Using molecular simulations to develop reliable design tools and correlations for engineering applications of aqueous electrolyte solutions. J. Chem. Eng. Data **61**, 1578–1584 (2016)

Hou, D., Li, T.: Influence of aluminates on the structure and dynamics of water and ions in the nanometer channel of calcium silicate hydrate (C-S-H) gel. Phys. Chem. Chem. Phys. **20**, 2373–2387 (2018)

Hwang, D.W., Sinha, A.K., Cheng, C.-Y., Yu, T.-Y., Hwang, L.-P.: Water dynamics on the surface of MCM-41 via ^2H double quantum filtered NMR and relaxation measurements. J. Phys. Chem. B **105**, 5713–5721 (2001)

Icaza, J.C., Guduru, R.K.: Effect of ion charges on the electric double layer capacitance of activated carbon in aqueous electrolyte systems. J. Power Sources **336**, 360–366 (2016)

Kalluri, R.K., Biener, M.M., Suss, M.E., Merrill, M.D., Stadermann, M., Santiago, J.G., Baumann, T.F., Biener, J., Striolo, A.: Unraveling the potential and pore-size dependent capacitance of slit-shaped graphitic carbon pores in aqueous electrolytes. Phys. Chem. Chem. Phys. **15**, 2309–2320 (2013)

Leng, Y.: Hydration force and dynamic squeeze-out of hydration water under subnanometer confinement. J. Phys.: Condens. Matter. **20**, 354017 (2008)

Mähler, J., Persson, I.: A study of the hydration of the alkali metal ions in aqueous solution. Inorg. Chem. **51**, 425–438 (2012)

Malan, A., Ayappa, K.G., Murad, S.: Effect of confinement on the hydration and solubility of NaCl in water. Chem. Phys. Lett. **431**, 88–93 (2006)

Nishi, M., Ohkubo, T., Tsurusaki, K., Itadani, A., Ahmmad, B., Urita, K., Moriguchi, I., Kittaka, S., Kuroda, Y.: Highly compressed nanosolution restricted in cylindrical carbon nanospaces. Nanoscale **5**, 2080–2088 (2013)

Ohba, T.: Anomalously enhanced hydration of aqueous electrolyte solution in hydrophobic carbon nanotubes to maintain stability. ChemPhysChem **15**, 415–419 (2014)

Ohba, T.: Water assistance in ion transfer during charge and discharge cycles. J. Phys. Chem. C **119**, 15185–15194 (2015)

Ohba, T.: Fast ion transportation associated with recovering hydration shells in a nanoelectrolyte between conical carbon nanopores during charging cycles. J. Phys. Chem. C **121**, 10439–10444 (2017)

Ohba, T., Kojima, N., Kanoh, H., Kaneko, K.: Unique hydrogen-bonded structure of water around Ca ions confined in carbon slit pores. J. Phys. Chem. C **113**, 12622–12624 (2009)

Ohba, T., Hata, K., Kanoh, H.: Significant hydration shell formation instead of hydrogen bonds in nanoconfined aqueous electrolyte solutions. J. Am. Chem. Soc. **134**, 17850–17853 (2012)

Ohkubo, T., Konishi, T., Hattori, Y., Kanoh, H., Fujikawa, T., Kaneko, K.: Restricted hydration structures of Rb and Br ions confined in slit-shaped carbon nanospace. J. Am. Chem. Soc. **124**, 11860–11861 (2002)

Ohkubo, T., Hattori, Y., Kanoh, H., Konishi, T., Fujikawa, T., Kaneko, K.: Structural anomalies of Rb and Br ionic nanosolutions in hydrophobic slit-shaped solid space as revealed by the EXAFS technique. J. Phys. Chem. B **107**, 13616–13622 (2003)

Ohkubo, T., Nishi, M., Kuroda, Y.: Actual structure of dissolved zinc ion restricted in less than 1 nanometer micropores of carbon. J. Phys. Chem. C **115**, 14954–14959 (2011)

Ohkubo, T., Takehara, Y., Kuroda, Y.: Water-initiated ordering around a copper ion of copper acetate confined in slit-shaped carbon micropores. Microporous Mesoporous Mater. **154**, 82–86 (2012)

Ohkubo, T., Kusudo, T., Kuroda, Y.: Asymmetric hydration structure around calcium ion restricted in micropores fabricated in activated carbons. J. Phys.: Condens. Matter **28**, 464003 (2016)

Oya, Y., Hata, K., Ohba, T.: Interruption of hydrogen bonding networks of water in carbon nanotubes due to strong hydration shell formation. Langmuir **33**, 11120–11125 (2017)

Pfeifer, J.R., Reiß, P., Koert, U.: Crown ether-gramicidin hybrid ion channels: dehydration-assisted ion selectivity. Angew. Chem., Int. Ed. **45**, 501–504 (2006)

Qiu, Y., Ma, J., Chen, Y.: Ionic behavior in highly concentrated aqueous solutions nanoconfined between discretely charged silicon surfaces. Langmuir **32**, 4806–4814 (2016)

Richards, L.A., Schafer, A.I., Richards, B.S., Corry, B.: The importance of dehydration in determining ion transport in narrow pores. Small **8**, 1701–1709 (2012)

Samoilov, O.Y.: A new approach to the study of hydration of ions in aqueous solutions. Discuss Faraday Soc. **24**, 141–146 (1957)

Shimizu, A., Taniguchi, Y.: NMR studies on the rotational motion of coordinated D_2O molecules in MBr ($M = Li^+$, Na^+, K^+, Cs^+) dilute aqueous solutions. Bull. Chem. Soc. Jpn. **63**, 1572–1577 (1990)

Takahara, S., Nakano, M., Kittaka, S., Kuroda, Y., Mori, T., Hamano, H., Yamaguchi, T.: Neutron scattering study on dynamics of water molecules in MCM-41. J. Phys. Chem. B **103**, 5814–5819 (1999)

Ueda, T., Omichi, H., Chen, Y., Kobayashi, H., Kubota, O., Miyakubo, K., Eguchi, T.: ^2H NMR study of 2D melting and dynamic behaviour of $CDCl_3$ confined in ACF nanospace. Phys. Chem. Chem. Phys. **12**, 9222–9229 (2010)

Uedaira, H., Uedaira, H.: Nuclear magnetic relaxations of ^2H and ^{23}Na in aqueous solutions of sodium sulfonates. Nippon Kagaku Kaishi **1986**, 1265–1269 (1986)

Uedaira, H., Ikura, M., Uedaira, H.: Natural-abundance oxygen-17 magnetic relaxation in aqueous solutions of carbohydrates. Bull. Chem. Soc. Jpn **62**, 1–4 (1989)

Urita, K., Ide, N., Isobe, K., Furukawa, H., Moriguchi, I.: Enhanced electric double-layer capacitance by desolvation of lithium ions in confined nanospaces of microporous carbon. ACS Nano **8**, 3614–3619 (2014)

Wu, X., Lu, L., Zhu, Y., Zhang, Y., Lu, X.: Ionic hydration of Na^+ inside carbon nanotubes under electric fields. Fluid Phase Equilib. **353**, 1–6 (2013)

Yu, H., Noskov, S.Y., Roux, B.: Hydration number, topological control, and ion selectivity. J. Phys. Chem. B **113**, 8725–8730 (2009)

Zhou, V., Morais-Cabral, J.H., Kaufman, A., MacKinnon, R.: Chemistry of ion coordination and hydration revealed by a K^+ channel-Fab complex at 2.0 Å resolution. Nature **414**, 43–48 (2001)

Zhu, Y., Guo, X., Shao, Q., Wei, M., Lu, X.: Molecular simulation study of the effect of inner wall modified groups on ionic hydration confined in carbon nanotube. Fluid Phase Equilib. **297**, 215–220 (2010)